






Mad2 promotes Cyclin B2 recruitment to the kinetochore for guiding accurate mitotic checkpoint

Sikai Liu^{1,2}, Xiao Yuan^{1,2}, Ping Gui^{1,2} , Ran Liu^{1,2}, Olanrewaju Durojaye^{1,2}, Donald L Hill³, Chuanhai Fu^{1,2} , Xuebiao Yao^{1,*} , Zhen Dou^{1,2,**}  & Xing Liu^{1,2,***} 

Abstract

Accurate mitotic progression relies on the dynamic phosphorylation of multiple substrates by key mitotic kinases. Cyclin-dependent kinase 1 is a master kinase that coordinates mitotic progression and requires its regulatory subunit Cyclin B to ensure full kinase activity and substrate specificity. The function of Cyclin B2, which is a closely related family member of Cyclin B1, remains largely elusive. Here, we show that Mad2 promotes the kinetochore localization of Cyclin B2 and that their interaction at the kinetochores guides accurate chromosome segregation. Our biochemical analyses have characterized the Mad2-Cyclin B2 interaction and delineated a novel Mad2-interacting motif (MIM) on Cyclin B2. The functional importance of the Cyclin B2-Mad2 interaction was demonstrated by real-time imaging in which MIM-deficient mutant Cyclin B2 failed to rescue the chromosomal segregation defects. Taken together, we have delineated a previously undefined function of Cyclin B2 at the kinetochore and have established, in human cells, a mechanism of action by which Mad2 contributes to the spindle checkpoint.

Keywords cyclin B2; kinetochore; Mad2; mitosis; spindle assembly checkpoint

Subject Categories Cell Cycle

DOI 10.15252/embr.202154171 | Received 17 October 2021 | Revised 8 March 2022 | Accepted 15 March 2022 | Published online 5 April 2022

EMBO Reports (2022) 23: e54171

Introduction

Mitotic entry is triggered by activation of a mitotic kinase network centered on cyclin-dependent kinase 1 (Cdk1) and the simultaneous repression of Cdk1-opposing phosphatases. The general framework of Cdk1 activation and its role in mitotic entry is well-established (Crnec & Hohegger, 2019). Beyond mitotic entry, Cdk1-Cyclin B

has multiple functions, including nuclear envelope breakdown (NEBD), chromosome condensation, kinetochore assembly, establishing correct kinetochore-microtubule attachment, regulating the spindle assembly checkpoint (SAC) function, and inhibiting separate activity (Nigg, 2001; Hohegger *et al.*, 2008; Yu & Yao, 2008; Gascoigne & Cheeseman, 2013; Mo *et al.*, 2016; Hara & Fukagawa, 2018; Hayward *et al.*, 2019b; Yu *et al.*, 2021). SAC is a cell-cycle surveillance mechanism that safeguards against erroneous chromosomal segregation. In the presence of improper kinetochore-microtubule attachment, SAC senses it and precludes the entry into anaphase (Musacchio, 2015; Dou *et al.*, 2019). Mounting evidence suggests that Cdk1 activity is directly involved in SAC function. Sustained Cdk1 activity is required to keep *Xenopus* egg extracts in a mitotic state (D'Angiolella *et al.*, 2003). Using the selective Cdk1 inhibitor RO-3306, Cdk1 activity was proved to be essential for maintaining the mitotic state and for preventing premature cytokinesis (Vassilev *et al.*, 2006). Later, studies demonstrated that inactivation of Cdk1-Cyclin B is a prerequisite for the silence of SAC in early anaphase, supporting that Cdk1-Cyclin B is an intrinsic component of SAC signaling (Clijsters *et al.*, 2014; Rattani *et al.*, 2014; Vazquez-Novelle *et al.*, 2014).

In vertebrates, there are three Cyclin B members: Cyclin B1, B2, and B3 (Malumbres & Barbacid, 2005). Both Cyclin B1 and B2 are expressed in somatic cells, whereas Cyclin B3 expression is confined to germ cells (Satyanarayana & Kaldis, 2009; Karasu *et al.*, 2019). Human Cyclin B1 localizes at the centrosome in the G2 phase and at kinetochores in the prometaphase (Bentley *et al.*, 2007; Chen *et al.*, 2008). However, recently, the importance and molecular basis of Cyclin B1 kinetochore localization has begun to be appreciated. Recent work from Barr and colleagues has established the Cyclin B1-Mad1 interaction and has revealed the role of Cyclin B1 as a *bona fide* SAC component (Alfonso-Perez *et al.*, 2019). A study by Saurin group's showed that Cyclin B1 scaffolds the kinetochore corona localization of Mad1 and ensures a robust SAC signal (Allan *et al.*, 2020). Further, a study from Pines' group demonstrated that

1 MOE Key Laboratory for Cellular Dynamics and The First Affiliated Hospital, School of Life Sciences, University of Science and Technology of China, Hefei, China

2 CAS Center for Excellence in Molecular Cell Science, Chinese Academy of Sciences, Shanghai, China

3 Comprehensive Cancer Center, University of Alabama at Birmingham, Birmingham, AL, USA

*Corresponding author. Tel: +86 551 63606304; Fax: +86 551 63607141; E-mail: yaobx@ustc.edu.cn

**Corresponding author. Tel: +86 551 63606304; Fax: +86 551 63607141; E-mail: douzhen@ustc.edu.cn

***Corresponding author (Lead contact). Tel: +86 551 63606304; Fax: +86 551 63607141; E-mail: xing1017@ustc.edu.cn

Mad1 recruits Cyclin B1-Cdk1 to nuclear pores. In turn, Cyclin B1-Cdk1 promotes Mad1 translocation to kinetochores from nuclear pores (Jackman *et al.*, 2020). Despite some inconsistencies, these three independent studies demonstrated the importance of Cyclin B1 kinetochore localization in robust SAC signaling (Houston *et al.*, 2020).

Although the function of Cyclin B1 was extensively studied, the precise role of Cyclin B2 remains elusive. An early study from Nigg's lab showed that expression of a nondegradable chicken Cyclin B2 mutant in HeLa cells causes mitotic arrest (Gallant & Nigg, 1992). Cyclin B1 knock-out mice are embryonic lethal. However, Cyclin B2-null mice are viable and largely normal but with somewhat reduced body size (Brandeis *et al.*, 1998). Recently, evidence challenged the viewpoint that Cyclin B2 is dispensable in mammals. Compared with Cyclin B1 single knockdown cells, Cyclin B1 and B2 double knockdown cells displayed more severe SAC defects, indicating that Cyclin B2 participates in the SAC function in parallel with Cyclin B1 (Gong & Ferrell, 2010). In mouse oocytes, Hec1 stabilizes the Cyclin B2 protein and hence regulates the G2-M transition and early prometaphase (Gui & Homer, 2013). Overexpression of either Cyclin B1 or Cyclin B2 causes aneuploidy and drives tumorigenesis, but through different mechanisms. Moreover, endogenously expressed Cyclin B2 and p53 act antagonistically on Aurora A to control faithful centrosome separation and chromosome segregation (Nam & van Deursen, 2014). Consistent with the high expression in prophase arrest oocytes, in mouse oocytes, Cyclin B2 is required for progression through meiosis (Daldello *et al.*, 2019). Conditional knock-out experiments reveal that, in oocyte meiosis I, Cyclin B2 compensates for Cyclin B1 (Li *et al.*, 2018). In addition, like Cyclin B1/Cdk1, the Cyclin B2/Cdk1 complex conservatively inhibits separase activity in oocyte meiosis (Li *et al.*, 2021).

The protein domain organization and size of Cyclins B1 and B2 are similar. However, whether Cyclin B2 also localizes at kinetochore and participates in the SAC function remains unknown. Here, we examined the localization and function of human Cyclin B2. We found that, like Cyclin B1, Cyclin B2 localizes at kinetochores in prometaphase cells. Of note, the kinetochore receptor for Cyclin B2 is not Mad1, but Mad2. The direct binding of Cyclin B2 to Mad2 depends on the C-terminal Mad2-interacting motif (MIM) of Cyclin B2. Expression of Mad2-binding deficient Cyclin B2 results in an elevation of chromosome segregation defects, due to aberrant SAC signaling. We reason that the kinetochore-localized Cyclin B2 acts in parallel with Cyclin B1 to ensure the robust SAC function and faithful mitotic chromosome segregation.

Results

Cyclin B2 localizes at unaligned kinetochores in prometaphase cells

Human Cyclin B1 localizes in the cytoplasm and centrosomes in interphase cells and re-localizes to spindle poles and kinetochores in prometaphase cells (Draviam *et al.*, 2001; Jackman *et al.*, 2003; Bentley *et al.*, 2007; Chen *et al.*, 2008; Alfonso-Perez *et al.*, 2019). Considering the similar protein domain organization of human Cyclin B1 and B2 (see Fig 1A for schematic representation), we asked whether

Cyclin B2 also localizes at kinetochores and participates in the SAC function. To this end, we examined the localization of endogenous Cyclin B2 through immunofluorescence staining using a commercial Cyclin B2 antibody (abcam, ab185622). As shown in Fig 1B (top row), Cyclin B2 localizes at the nuclear envelope in prophase cells. Co-staining the nuclear envelope marker mAb414 confirmed nuclear envelope localization of Cyclin B2 in prophase (Fig 1C). After NEBD, it was apparent that Cyclin B2 localizes at kinetochores in prometaphase cells (Fig 1B, second row). As expected, the Cyclin B2 kinetochore signal diminished, but with spindle pole distribution in metaphase cells (Fig 1B, third row), it was undetectable in anaphase cells (Fig 1B, bottom row). As shown in Fig 1D, the immunofluorescence staining for Cyclin B2 is specific since siRNA treatment to suppress Cyclin B2 eliminated the kinetochore signal of Cyclin B2, but Cyclin B2 localization to kinetochore remained in cells transfected with Cyclin B1 siRNA. If endogenous Cyclin B2 is kinetochore-associated, exogenously expressed Cyclin B2 should also localize to the kinetochore. Thus, we engineered HeLa cells to stably express EGFP-tagged Cyclin B2. As shown in Fig EV1A, Western blotting analyses using GFP antibody proved the correct expression of GFP-Cyclin B2. In addition, the expression level of GFP-Cyclin B1/B2 was comparable with endogenous Cyclin B1/B2 (Fig EV1B). As predicted, the cell-cycle-dependent distribution pattern of GFP-Cyclin B2 was consistent with that of the endogenous protein labeled with an anti-Cyclin B2 antibody (Fig EV1C). Further, the subcellular localization pattern of GFP-Cyclin B2 was similar to that of cells expressing GFP-Cyclin B1 (Fig EV1D). Similar with Cyclin B1, Cyclin B2 localized mainly in the cytoplasm in interphase. However, inconsistent with a previous report, no co-localization of Cyclin B2 with the Golgi complex was evident (Fig EV1E) (Jackman *et al.*, 1995). We also observed centrosome localization of Cyclin B2 in interphase cells, as shown by the co-localization with centrosome protein, pericentrin (Fig EV1F).

We next examined the localization of Cyclin B2 in cells challenged with various microtubule poisons to activate the spindle checkpoint. As shown in Fig 1E, Cyclin B2 localizes at unattached kinetochores (nocodazole-treated cells), syntelically attached kinetochores (STLC-treated cells) and kinetochores without proper tension (taxol-treated cells). Cyclin B1 expression peaks in mitosis, and the Cyclin B1 protein undergoes APC/C-dependent degradation during mitotic exit. We next asked whether Cyclin B2 has a similar protein expression profile with Cyclin B1. To this end, double thymidine synchronized cells were released and collected at selected time points. The cell lysates were analyzed by Western blots using Cyclin B1/B2 antibody. In agreement with Cyclin B1, Cyclin B2 peaked at early mitotic phase and decreased after mitotic exit (Fig 1F). We further measured the expression of Cyclin B2 in HCT116 and HeLa cells. As predicted, Cyclin B2 protein levels were elevated in mitotic HCT116 and HeLa cells (Fig EV1G). Thus, we conclude that Cyclin B2 localizes at the centrosome in G2 phase, at the nuclear envelope in prophase, and at unattached kinetochores in prometaphase.

Cyclin B2 kinetochore localization depends on Mad2

We next sought to identify the proteins underlying the kinetochore localization of Cyclin B2. Considering that Mps1 and Aurora B lie

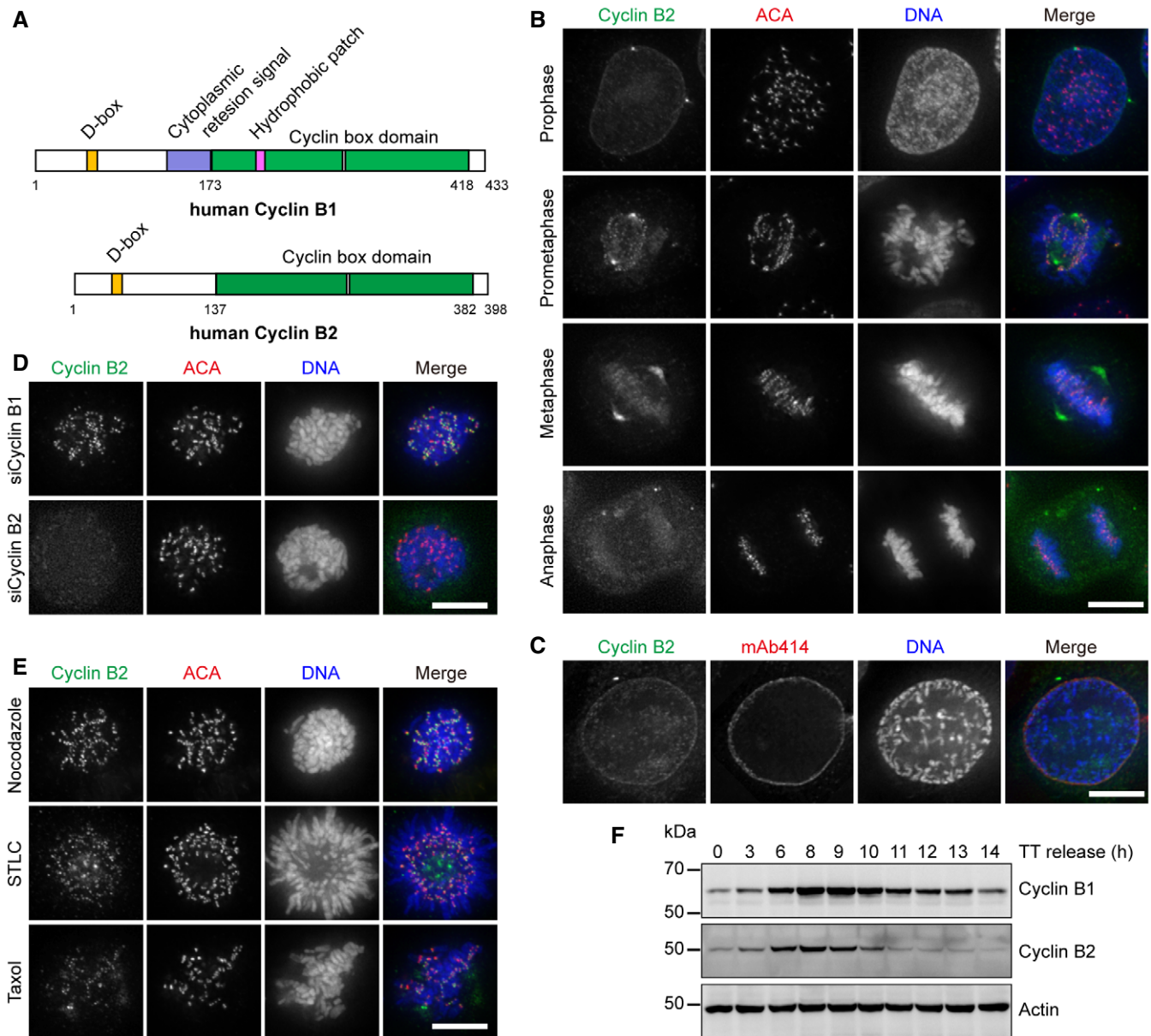


Figure 1. Cyclin B2 localizes at unaligned kinetochores in HeLa cells.

- A** Schematic representation of human Cyclin B1 and Cyclin B2 protein domain organization.
- B** Representative immunofluorescence images of HeLa cells in various mitotic stages. Cells were extracted, fixed, and co-stained for Cyclin B2 (green), ACA (red), and DNA (blue). Scale bar, 10 μ m.
- C** Representative immunofluorescence images of HeLa cells that were fixed and co-stained for Cyclin B2 (green), mAb414 (red), and DNA (blue). Scale bar, 10 μ m.
- D, E** Representative immunofluorescence images of HeLa cells treated with an indicated siRNA (D) or various drugs (E). Cells were extracted, fixed, and co-stained for Cyclin B2 (green), ACA (red), and DNA (blue). Scale bar, 10 μ m.
- F** HeLa cells were synchronized by double thymidine, then released and collected at selected time points. Cell lysate samples were resolved by SDS-PAGE and analyzed by Western blotting using anti-Cyclin B1 antibody, anti-Cyclin B2 antibody, or anti- β -Actin antibody.

Source data are available online for this figure.

upstream of SAC signaling (Santaguida *et al.*, 2011; Saurin *et al.*, 2011; Pachis & Kops, 2018; Gui *et al.*, 2020), we tested whether Cyclin B2 kinetochore localization was sensitive to Mps1, Aurora B, and Cdk1 kinase activity. As shown in Fig EV2A and B, the Cyclin B2 kinetochore signal was diminished in cells treated with the Mps1

inhibitor, reversine, or the Aurora B inhibitor, hesperadin (Hauf *et al.*, 2003; Santaguida *et al.*, 2010). In addition, the Cyclin B2 signal at the kinetochore was moderately lower in cells treated with the Cdk1 inhibitor, RO-3306. These results suggest that Cyclin B2 kinetochore localization relies on Cdk1 kinase activity.

To identify the proteins responsible for Cyclin B2 localization at the kinetochore, we carried out an immunoprecipitation coupled to mass spectrometric analysis. To this end, Flag-tagged Cyclin B1 and Flag-tagged B2-bound Sepharose beads were used as an affinity matrix to incubate with mitotic HeLa cell lysates. After extensive washes, the proteins bound to the beads were analyzed by mass spectrometry. In agreement with recent reports (Alfonso-Perez *et al*, 2019; Allan *et al*, 2020; Jackman *et al*, 2020), the Mad1 score ranks highest among the Cyclin B1-binding partners identified (Fig 2A). Cdk1, Cdk2, Cdk5, and several APC/C subunits were also detected in Cyclin B1 immunoprecipitates. To our surprise, Mad1 was not identified in Cyclin B2 immunoprecipitates. Instead, Mad2, the core SAC factor and Mad1 binding partner (Li & Benenzra, 1996; Lara-Gonzalez *et al*, 2021), was identified as a Cyclin B2-binding protein (Fig 2A and Datasets EV1–EV4).

To verify the direct binding between Cyclin B2 and Mad2, we performed a co-immunoprecipitation assay. The Mad2 signal was detected in Cyclin B2 immunoprecipitates using two different commercial antibodies (Fig 2B). Mad2 transforms from the cytoplasmic open conformation (O-Mad2) to the closed conformation (C-Mad2) when is bound to the kinetochore Mad1-Mad2 heteotetramer (Mapelli *et al*, 2007; Luo & Yu, 2008). To test whether Cyclin B2 selectively binds with O-Mad2 or C-Mad2, Flag-tagged Mad2 wild-type (WT), Δ C mutant (O-Mad2), and L13A mutant (C-Mad2) were used as affinity matrices to absorb mitotic HeLa lysates. Indeed, all three Mad2 proteins bound endogenous Cyclin B2 (Fig EV2C). Further, C-Mad2 precipitated more Cyclin B2 protein, suggesting a stronger binding affinity. Furthermore, we tested whether C-Mad2 also binds Cyclin B1. As shown in Fig 2C, Cyclin B2, but not Cyclin B1, was absorbed by C-Mad2 affinity matrix. In contrast, Cyclin B1, but not Cyclin B2, was detected in Mad1 immunoprecipitates (Fig 2D). Next, we also performed a GST pulldown assay to verify the direct physical interaction between Mad2 and Cyclin B2. As a result, GST-tagged Cyclin B2 (the cyclin box domain) pulled down recombinant C-Mad2 proteins. In contrast, Cyclin B1 (the cyclin box domain) failed to pull down Mad2 protein (Fig 2E). Thus, the results show that the Mad2-Cyclin B2 interaction is specific and also confirm the Mad1-Cyclin B1 interaction.

We next examined the subcellular co-localization of Cyclin B2 and Mad2. Endogenous Cyclin B2 displayed an exact overlay with Mad2 at the kinetochores (Fig EV2D and E). Subsequently, we tested whether the localization of Cyclin B2 depends on Mad2. Compared with cells treated with control siRNA, the Cyclin B2 signal at the kinetochores declined in GFP-Cyclin B2-stable cells transfected with siMad2 (Fig 2F and G). However, the Cyclin B1 kinetochore signal remained unchanged in GFP-Cyclin B1-stable cells treated with siControl or siMad2 (Fig 2H and I), suggesting that Cyclin B1 distribution is independent of Mad2. The siMad2 efficiency was confirmed by Western blots and immunofluorescence staining (Fig EV2F–H). Thus, we concluded that the kinetochore localization of Cyclin B2 depends on Mad2. We further examined whether the localization of Cyclin B2 depends on Mad1. As shown (Fig EV3A–D), the kinetochore signals of both Cyclin B1 and Cyclin B2 disappeared in cells depleted of Mad1, indicating that Mad1 is essential for the kinetochore localization of Cyclin B1 and Cyclin B2.

Cyclin B2 binds Mad2 directly through its MIM

Mad2 is a key component of the mitotic checkpoint complex (MCC), which directly inhibits the ubiquitin E3 ligase activity of APC/C. Several Mad2-binding partners, such as Mad1, Cdc20, Shugoshin, and insulin receptor, contain a motif called Mad2-interacting motif (MIM) (Luo *et al*, 2002; Orth *et al*, 2011; Choi *et al*, 2016). To examine whether Cyclin B2 binds Mad2 using the same motif, we conducted a protein sequence alignment analysis. As expected, a sequence conformed to the MIM motif (K Φ F Φ x Φ xxxP) was identified in human Cyclin B2 (aa. 372–380). Two key residues within the corresponding sequence in Cyclin B1 were divergent (Fig 3A). To test the role of MIM in mediating Cyclin B2 kinetochore localization, a Cyclin B2 mutant (K372A-L373A-L374A-I376A, named as Cyclin B2^{MIM-4A}) was generated. We then expressed Flag-tagged Cyclin B2^{WT}, Cyclin B2^{MIM-4A}, and Cyclin B1 in 293T cells and performed an immunoprecipitation assay. As shown in Fig 3B, compared with Cyclin B2^{WT}, Cyclin B2^{MIM-4A} pulled down a lower amount of endogenous Mad2. Since Cdk1 is the most important binding partner of Cyclin B2, we asked if the MIM motif is required for its

Figure 2. Mad2 recruits Cyclin B2 to kinetochores.

- A Table showing the proteins binding to Cyclin B1 and Cyclin B2 identified by immunoprecipitation and subsequent mass spectrometry. In brief, Flag-Cyclin B1 and Flag-Cyclin B2 were expressed in 293T cells and immunoprecipitated with anti-Flag M2 beads. Then Cyclin B1/B2-bound beads were incubated with pre-cleared mitotic HeLa cell lysates. The immunoprecipitates were analyzed by mass spectrometry.
- B Immunoprecipitation assay performed with two different rabbit Cyclin B2 antibodies. Nocodazole-arrested mitotic cells were collected and lysed. Immunoprecipitation was accomplished using control IgG, anti-Cyclin B2-1 (Abcam, ab185622), and anti-Cyclin B2-2 (Proteintech, 21644-1-AP). Immunoprecipitation samples were resolved by Western blotting using a mouse anti-Cyclin B2 antibody (Santa Cruz, sc-28303) and a mouse anti-Mad2 antibody (Santa Cruz, sc-47747).
- C, D Flag immunoprecipitation assay. 293T cells were co-transfected with Flag-C-Mad2 and GFP-Cyclin B1/B2 (C), and with Flag-Mad1-1-215 and GFP-Cyclin B1/B2 (D). After 36 h, the cells were collected and lysed, and immunoprecipitation was accomplished with anti-Flag M2 beads. Immunoprecipitates were resolved by SDS-PAGE and analyzed by Western blotting using anti-Flag antibody and anti-GFP antibody.
- E GST pulldown assay. Purified GST, GST-Cyclin B1-165-433, and GST-Cyclin B2-130-398-bound agarose beads were used as affinity matrices to absorb purified Trx-6 \times His-tagged C-Mad2 recombinant protein. Absorbed proteins were analyzed by SDS-PAGE and Coomassie Brilliant Blue staining.
- F–I Representative immunofluorescence images of HeLa cells stably-expressing GFP-Cyclin B2 (F) or GFP-Cyclin B1 (H). The cells were transfected with siControl or siMad2 for 36 h followed by treatment with nocodazole plus MG132 for 2 h. Cells were then fixed and co-stained for Mad2 (red) and DNA (blue). Scale bar, 10 μ m. Scatter graphs illustrating kinetochore intensity of GFP-Cyclin B2 (G) or GFP-Cyclin B1 (I) in cells treated as in F and H, respectively. Bars represent the mean kinetochore intensity (\pm SD) normalized to values of the siControl group. Each dot represents one cell (\geq 30 cells from three independent experiments). The Student's *t*-test was used to calculate *P*-values. *****P* < 0.0001; n.s., not significant.

Source data are available online for this figure.

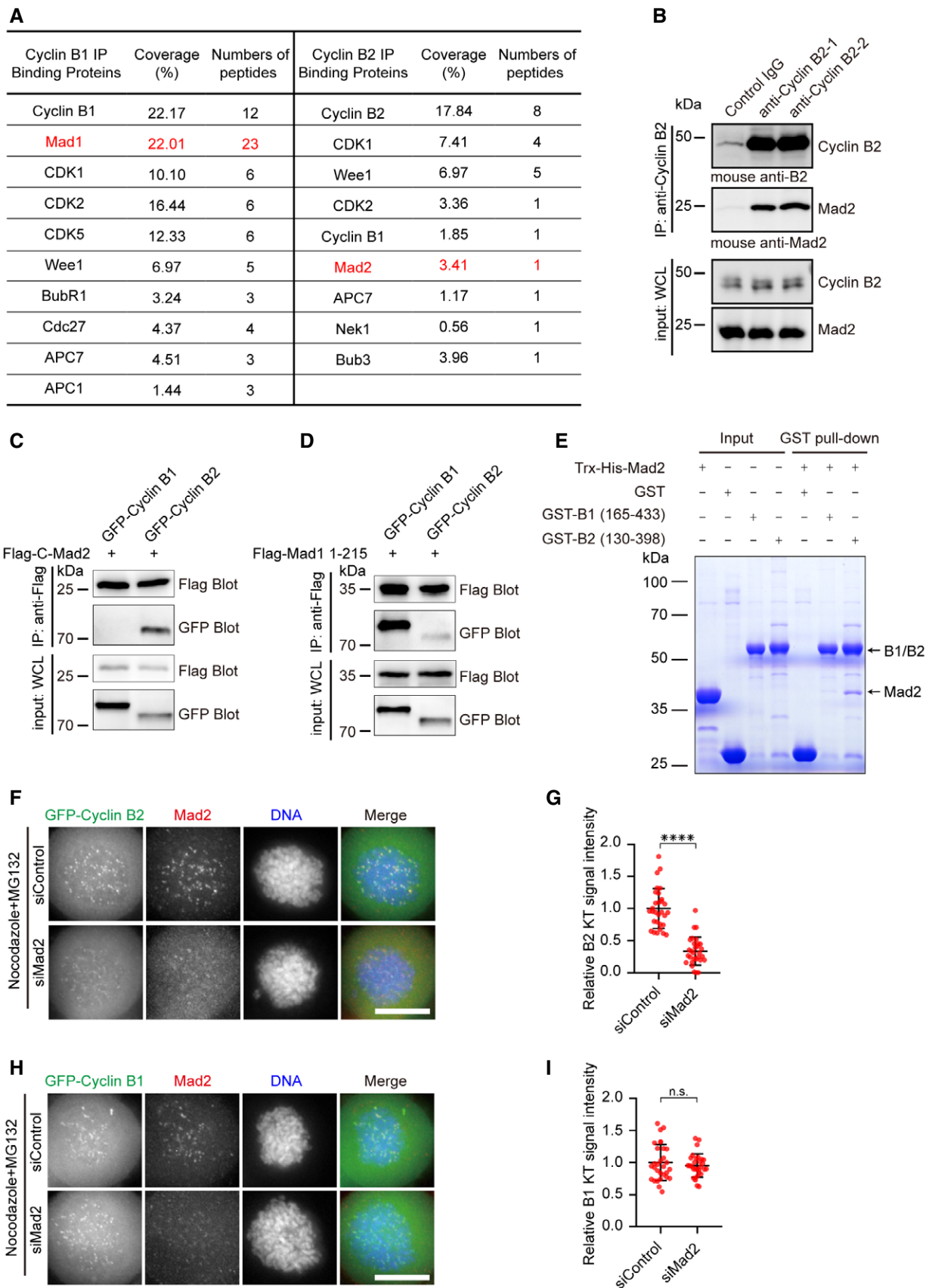


Figure 2.

binding with Cdk1. As a result, Flag-Cyclin B2^{WT} and Flag-Cyclin B2^{MIM-4A} pulled down an equivalent amount of Cdk1 (Fig 3C), suggesting that MIM is not involved in binding Cdk1.

We next examined the kinetochore localization of GFP-Cyclin B2^{MIM-4A}. Compared with GFP-Cyclin B2^{WT}, GFP-Cyclin B2^{MIM-4A} exhibited decreased kinetochore localization (Fig 3D and E). Thus,

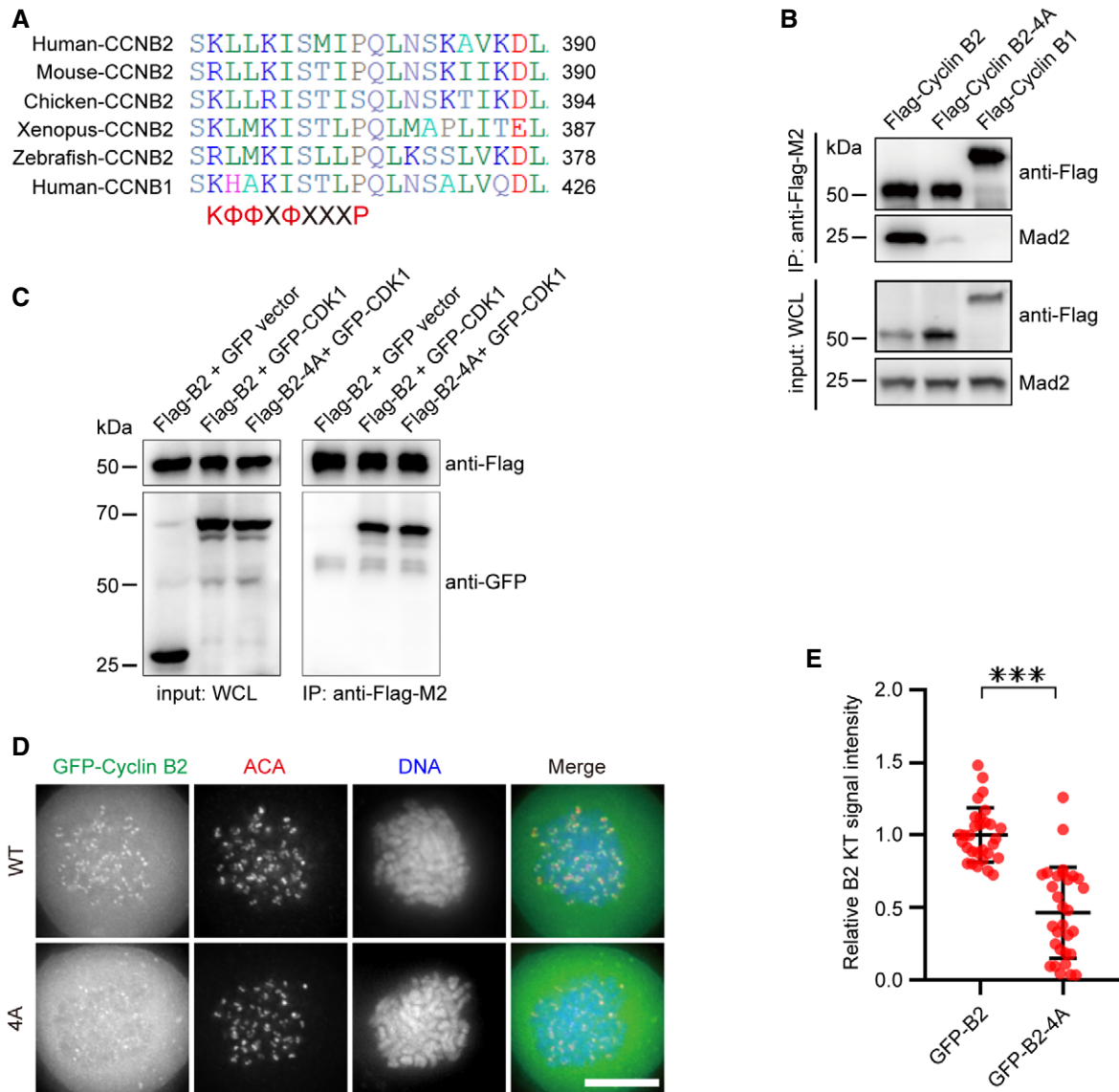


Figure 3. Cyclin B2 C-terminal MIM is required for its kinetochore localization.

- A Multiple sequence alignment of the Cyclin B2 and Cyclin B1 proteins from various species as indicated. The sequence alignment was developed by ClustalW2 software.
- B Flag immunoprecipitation assay. Flag-tagged Cyclin B2-WT, Cyclin B2-4A, or Cyclin B1 were expressed in 293T cells and purified with anti-Flag M2 beads. Subsequently, the beads were incubated with mitotic HeLa lysates for 2 h, and following extensive washes, immunoprecipitates were resolved by SDS-PAGE and analyzed by Western blotting using anti-Flag antibody and anti-Mad2 antibody.
- C Flag immunoprecipitation assay. 293T cells were co-transfected with Flag-Cyclin B2-WT or Flag-Cyclin B2-4A together with GFP (negative control) and GFP-CDK1. After 36 h, the cells were collected and lysed, and immunoprecipitation was accomplished with anti-Flag M2 beads. Immunoprecipitation samples were resolved by SDS-PAGE and analyzed by Western blotting using anti-GFP antibody and anti-Flag antibody.
- D Representative immunofluorescence images of HeLa cells transfected with GFP-Cyclin B2-WT or GFP-Cyclin B2-4A. After 36 h of transfection, cells were treated with nocodazole for 2 h. Then cells were fixed and co-stained for ACA (red) and DNA (blue). Scale bar, 10 μ m.
- E Scatter graphs illustrating kinetochore intensity of GFP-Cyclin B2-WT/4A treated as in D. Bars represent the mean kinetochore intensity (\pm SD) normalized to the values of GFP-Cyclin B2-WT. Each dot represents one cell (\geq 30 cells from three independent experiments). The Student's t-test was used to calculate P-values. *** $p < 0.001$.

Source data are available online for this figure.

we conclude that the MIM-mediated Cyclin B2-Mad2 interaction is essential for Cyclin B2 kinetochore localization.

The kinetochore localization of Cyclin B2 is essential for robust SAC signaling and accurate mitosis

To evaluate the function of Cyclin B2, we applied an siRNA to knock down Cyclin B2 protein and examined the phenotype using live-cell imaging. As shown in Fig 4A, the siRNA against Cyclin B2 was potent and specific. Most HeLa cells transfected with control siRNA entered anaphase with correct chromosome segregation. However, nearly 45% of cells transfected with siCyclin B2 displayed anaphase lagging chromosomes or chromosome bridges (Fig 4B and C). siCyclin B2-treated cells spent a similar time as control cells to enter anaphase from NEBD (Fig 4D). In addition, 5% of HCT116 cells treated with control siRNA contained anaphase lagging chromosomes. In contrast, with knocked-down Cyclin B2, 35% of HCT116 cells in anaphase displayed lagging chromosomes or chromosome bridges (Fig EV4A and B). We next constructed an siRNA-resistant GFP-Cyclin B2 plasmid and performed a rescue experiment after knocking down Cyclin B2. As shown in Fig 4E and F, most cells expressing GFP-Cyclin B2 finished correct mitotic progression. However, more than 50% of cells re-expressing GFP-Cyclin B2-4A entered anaphase in the presence of lagging chromosomes, suggesting compromised SAC signaling.

To verify that SAC signaling is compromised in Cyclin B2-depleted cells, we performed immunofluorescence assays to examine the kinetochore localization of key SAC factors such as Mad2 and Cdc20. As a result, the kinetochore signal intensity of Mad2 was lower in Cyclin B2 knockdown cells (Fig 5A and C). Further, we quantified the kinetochore localization of Mad2 in cells rescued with siRNA-resistant GFP-Cyclin B2-WT/4A. The Mad2 signal was evident in cells expressing GFP-Cyclin B2-WT but not in cells expressing GFP-Cyclin B2-4A (Fig 5B and C). The kinetochore signal of Cdc20 was also diminished in cells depleted of Cyclin B2 (Fig 5D and F). Similarly, re-expressing GFP-Cyclin B2-WT, but not GFP-Cyclin B2-4A, rescued the kinetochore localization of Cdc20 in cells with depleted Cyclin B2 (Fig 5E and F). In addition to Mad2 and Cdc20, other SAC factors such as Mad1, BubR1, and Bub1 also displayed moderately reduced kinetochore signals in cells with Cyclin B2 knockdown (Fig EV5A–F).

Next, we quantified the mitotic index of Cyclin B2 knockdown cells challenged with the microtubule poison, nocodazole. At 12 h

after nocodazole treatment, more than 80% control cells were in the mitotic phase as determined by phosphohistone H3-positive staining. On the contrary, only 40% of Cyclin B2-depleted cells stayed in the mitotic phase (Fig 5G). Re-expressing GFP-Cyclin B2-WT, but not GFP-Cyclin B2-4A, elevated the mitotic index in Cyclin B2 knockdown cells treated with nocodazole (Fig 5G). To monitor the activity of SAC, we examined the assembly of MCC, a downstream effector of SAC. To this end, immunoprecipitation was performed using an anti-Cdc20 antibody in siControl and siCyclin B2-transfected cells. Comparable amounts of Cdc20 protein were precipitated in the control group and the Cyclin B2 knockdown group. However, compared with the control cells, lower amounts of BubR1, Bub3, and Mad2 were co-precipitated for Cyclin B2 knockdown cells (Fig 5H). We note that the reduced amount of MCC is not due to the change in cell-cycle profile, as Cyclin B1 levels are similar in cells transfected with siControl or siCyclin B2 (Fig EV5G). Thus, we conclude that Cyclin B2 is required for maintaining robust SAC signaling and faithful mitotic progression.

Discussion

Cdk1 is the master regulator of mitosis. To execute its multiple roles, Cdk1 must phosphorylate its numerous substrates in a spatiotemporally controlled manner. Kinases adopt different mechanisms, such as the structure of the kinase catalytic cleft, the kinase docking site, localization of the kinase, and system-level competition between substrates, to phosphorylate their substrates selectively (Ubersax & Ferrell, 2007; Xu et al, 2021). Cyclin B determines Cdk1 substrate selectivity through the docking domain and subcellular localization of Cdk1. The function and localization of Cyclin B1 have been extensively studied. However, the exact subcellular localization of Cyclin B2 and its function remains elusive.

In the present study, we demonstrated that human Cyclin B2 exhibits a spatiotemporal dynamic subcellular localization similar to Cyclin B1. During interphase, Cyclin B2 localizes in the cytoplasm and to the centrosome. Upon mitotic entry, Cyclin B2 translocates to the nuclear envelope and into the nucleus. Once the nuclear envelope breaks down, Cyclin B2 localizes to unattached or improperly attached kinetochores. As a consequence of SAC satisfaction, Cyclin B2 leaves the kinetochores and is degraded by the APC/C. In human cells, Cyclin B2 localizes to the Golgi complex (Jackman

Figure 4. Cyclin B2 kinetochore localization is required for faithful mitotic progression.

- A HeLa cells were transfected with siControl or siCyclin B2. At 36 h after transfection, cells were collected and lysed. The samples were resolved by SDS-PAGE and analyzed by Western blotting using anti-Cyclin B2 antibody, anti-Cyclin B1 antibody, and anti-tubulin antibody.
- B Representative stills illustrating mitotic progression in mCherry-H2B-expressed cells treated with Control siRNA or Cyclin B2 siRNA. Images were acquired at the indicated time points after the start of NEBD. The arrow indicates lagging chromosomes. Scale bar, 10 μ m.
- C Bar graph illustrating the percentage of cells with normal anaphase or with anaphase lagging chromosomes in cells treated as in B. Bars are mean \pm SD (\geq 30 cells from three independent experiments). The Student's *t*-test was used to calculate *P*-values. ****P* < 0.001.
- D Scatter graph of the time from NEBD to the beginning of anaphase in cells treated as in B (*n* = 30 cells). Bars indicate mean \pm SD. The Student's *t*-test was used to calculate *P*-values for comparison of siControl and siCyclin B2 cells; n.s., not significant.
- E Representative stills illustrating mitotic progression in mCherry-H2B-expressed cells depleted of endogenous Cyclin B2 and rescued with GFP-Cyclin B2-WT or GFP-Cyclin B2-4A. Images were acquired at the indicated time points after the start of NEBD. Arrows indicate a chromosome bridge. Scale bar, 10 μ m.
- F Bar graph illustrating the percentage of cells with normal anaphase and cells with anaphase lagging chromosomes in cells treated as in E. Bars are mean \pm SD (\geq 30 cells from three independent experiments). The Student's *t*-test was used to calculate *P*-values. ****P* < 0.001.

Source data are available online for this figure.

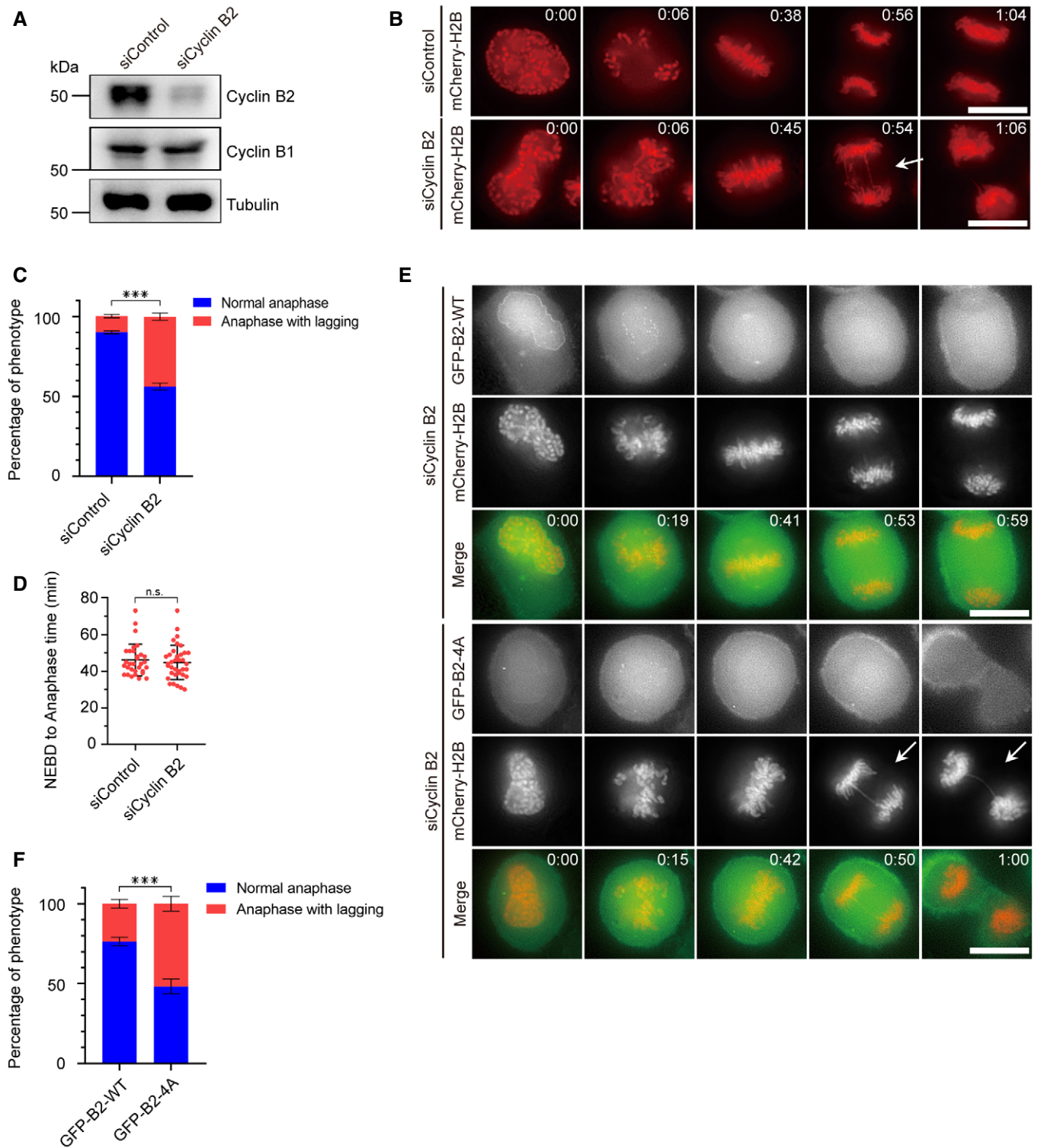


Figure 4.

et al, 1995). However, we did not observe any endogenous or exogenously expressed Cyclin B2 localized at the Golgi complex. Jackman and colleagues have reported that a small fraction of Cyclin B2 localizes to the spindle apparatus (Jackman *et al*, 1995), which is consistent with our observation. In addition, early work from Nigg's

laboratory showed that chicken Cyclin B2 localizes in the cytoplasm during interphase but translocates into the nucleus at the onset of mitosis (Gallant & Nigg, 1992).

The kinetochore localization of Cyclin B1 has been noted for years (Bentley *et al*, 2007; Chen *et al*, 2008). Until recently, the

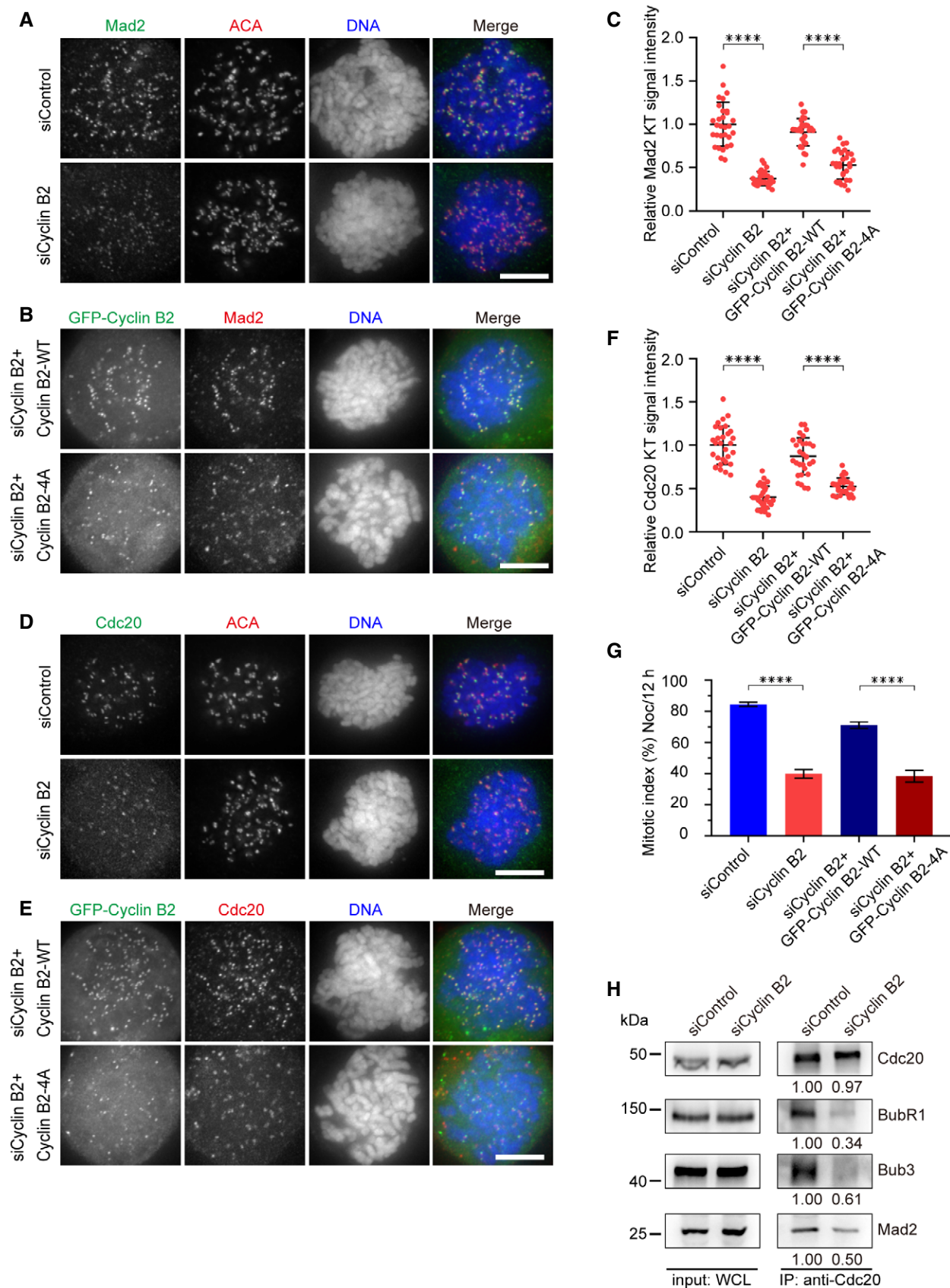


Figure 5.

Figure 5. Cyclin B2 is required for robust SAC signaling.

- A–F (A and D) Representative immunofluorescence images of HeLa cells transfected with siControl or siCyclin B2. After 36 h of transfection, cells were treated with nocodazole for 2 h. Then cells were fixed and co-stained for Mad2 (green) in A, Cdc20 (green) in D, ACA (red), and DNA (blue). Scale bar, 10 μ m. (B and E) Representative immunofluorescence images of HeLa cells co-transfected with siCyclin B2 plus GFP-tagged Cyclin B2-WT or Cyclin B2-4A. At 36-h post-transfection, cells were treated with nocodazole for 2 h. Cells were then fixed and co-stained for Mad2 (red) in B, Cdc20 (red) in E, and DNA (blue). Scale bar, 10 μ m. (C and F) Scatter graphs illustrating kinetochore intensity of Mad2 (C, cells treated as in A and B) and Cdc20 (F, cells treated as in D and E). Bars represent the mean kinetochore intensity (\pm SD) normalized to the values of the siControl group. Each dot represents one cell (\geq 30 cells from three independent experiments). The Student's *t*-test was used to calculate *P*-values. *****P* < 0.0001.
- G Bar graph illustrating the mitotic index in cells treated with low concentrations of nocodazole for 12 h. Values are mean \pm SD (\geq 1,000 cells from three independent experiments). The Student's *t*-test was used to calculate *P*-values. *****P* < 0.0001.
- H Immunoprecipitation assay performed with Cdc20 antibody. HeLa cells were transfected with siControl or siCyclin B2. At 36 h after transfection, cells were arrested in mitosis, collected, and lysed. Cell lysates were incubated with Protein A/G beads bound with Cdc20 antibody. Following extensive washes, immunoprecipitates were resolved by SAS-PAGE and analyzed by Western blotting using anti-Cdc20, anti-BubR1, anti-Bub3, and anti-Mad2 antibodies.

Source data are available online for this figure.

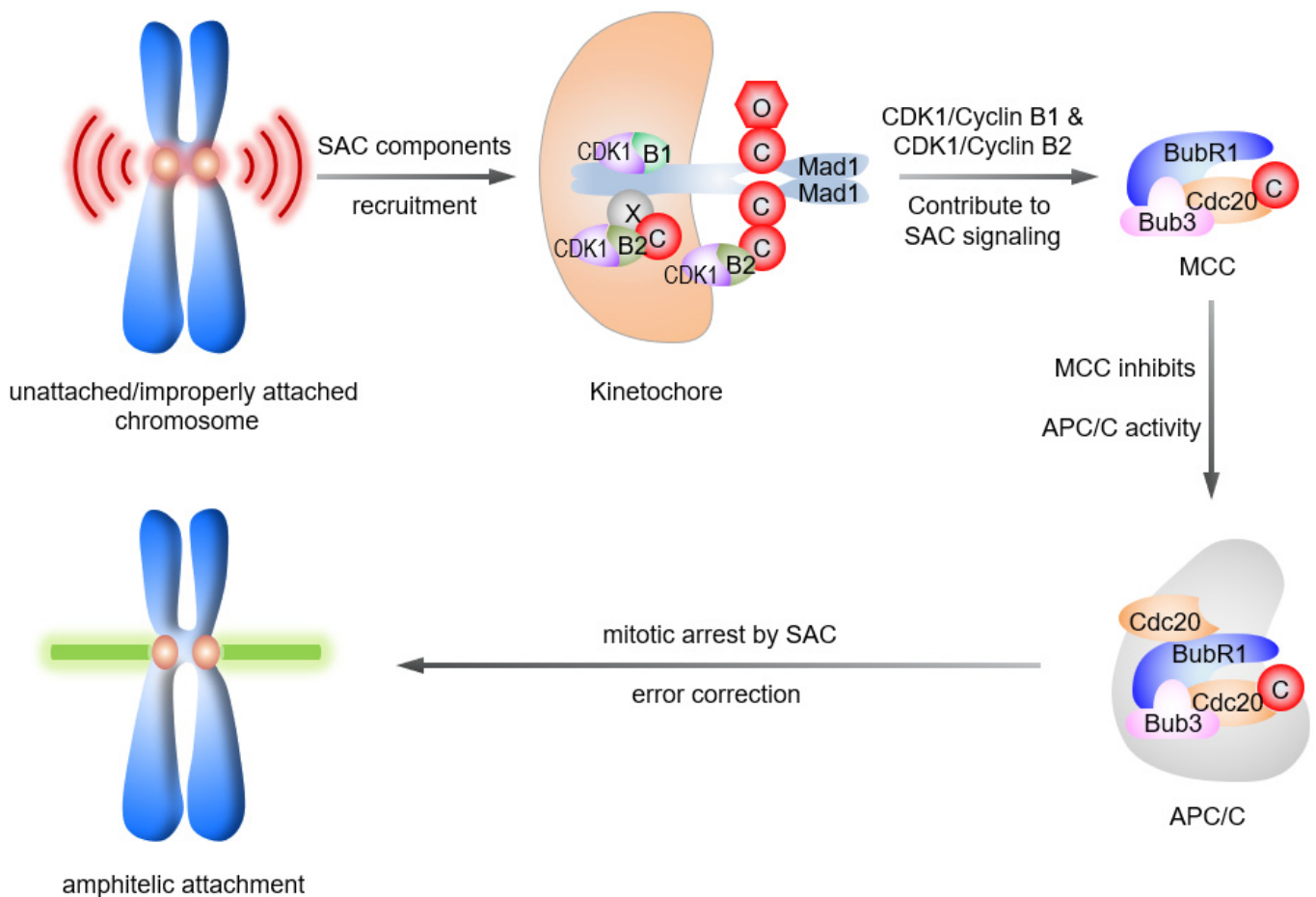


Figure 6. Working model to account for Cyclin B2 localization and function in mitosis.

After NEBD, Cyclin B2 localizes to unattached kinetochores, mediated by Mad2 bound to Mad1 or by Mad2 bound to a yet unidentified kinetochore receptor (protein-X). Multiple SAC factors, including kinases, localize at the outer kinetochores. Mad2-mediated Cyclin B2-Cdk1 contributes to SAC signaling, in complement with Mad1-mediated Cyclin B1-Cdk1. As a scaffold recruiting multiple SAC factors to the vicinity, the outer kinetochore catalyses the assembly of MCC. As a consequence, MCC inhibits the activity of APC/C to preclude the anaphase as long as improperly attached kinetochores are present. The error-correction machinery promotes the establishment of correct bipolar microtubule kinetochore attachment. When all kinetochores achieve bipolar attachment, SAC signaling is silenced, and the cell enters anaphase. C: C-Mad2, O: O-Mad2, X: protein-X, B1: Cyclin B1, B2: Cyclin B2.

molecular basis underlying Cyclin B1 kinetochore localization and its physiological functions was addressed by three groups (Alfonso-Perez *et al*, 2019; Allan *et al*, 2020; Jackman *et al*, 2020). Although

different functions were proposed, all three groups confirmed the Mad1-Cyclin B1 interaction (Houston *et al*, 2020). Since Cyclin B2 exhibits an identical localization pattern with that of Cyclin B1, it

was postulated that Mad1 interacts with and mediates Cyclin B2 kinetochore localization. Our experiments demonstrated that Mad2, but not Mad1, interacts with Cyclin B2. We further demonstrated that the Mad2-Cyclin B2 interaction was mediated by the MIM of Cyclin B2. In cells depleted of endogenous Cyclin B2, the MIM-deficient Cyclin B2 mutant failed to localize to the kinetochore effectively and rescue the mitotic defects.

Both Cyclin B1 and B2 are expressed in somatic tissues with a high proliferation ratio. It is widely believed that Cyclin B1 has an essential role for cell proliferation and that Cyclin B2 is dispensable, at least for mitosis. However, accumulating evidence supports that Cyclin B2 has a mitotic function, although in parallel with and complementary with Cyclin B1. Gong and co-workers found that Cyclin B1/B2 double-knockdown cells display a high incidence of late mitotic abnormalities (Gong *et al*, 2007; Gong & Ferrell, 2010). When Cyclin B2 is knocked down, numbers of HeLa cells with anaphase lagging chromosomes increase (Soni *et al*, 2008). Consistent with these results, we also observed a high frequency of anaphase lagging chromosomes in HeLa and HCT116 cells transfected with Cyclin B2 siRNA. We further demonstrated that the SAC function is impaired in cells with Cyclin B2 knockdown, as suggested by the decreased kinetochore localization of key SAC factors and decreased MCC assembly. Recently, Hochstrate and co-workers investigated the role of Cyclins A, B1, and B2 in RPE1 cells and concluded that Cyclin A is required for mitotic entry and that Cyclin B1/B2 is essential for accurate mitotic progression (Hegarar *et al*, 2020). No apparent SAC abrogation was observed in Cyclin B1/B2-depleted RPE1 cells, but the chromosome congression defect was severe. We reason that these observations highlight the difference between diploid cells and aneuploid cancer cells and support the idea that cancer cells are more dependent on SAC function for viability (Cohen-Sharir *et al*, 2021).

We demonstrated Mad2 is required for the kinetochore localization of Cyclin B2. However, decreased Mad2 (and Cdc20, BubR1, Bub1, and Mad1) localization at kinetochores was evident. A possible explanation is the reduced Cdk1 activity after knockdown of Cyclin B2 (Fig EV5H). Cdk1 phosphorylates Mps1 to activate the spindle checkpoint (Morin *et al*, 2012a; Hayward *et al*, 2019a). When Cyclin B2 was depleted, Cdk1 activity was reduced to lower Mps1 activity, which resulted in less kinetochore localization of Mad2 and Cdc20.

Our study favors a model indicating that the Mad2-mediated kinetochore localization of Cyclin B2 contributes to SAC signaling (Fig 6). In addition to inhibiting APC/C as a subunit of MCC, Mad2 has a novel function in recruiting Cyclin B2 to outer kinetochores. Kinetochore bound Mad1/Mad2 heterotetramer recruits an additional O-Mad2 and catalyses its conversion to C-Mad2. Prior studies have shown that C-Mad2 bound to a MIM ligand can no longer dimerize (Luo & Yu, 2008). Thus, it is likely C-Mad2 binds to a yet unidentified kinetochore receptor protein-X. Cyclin B2-Cdk1, in complement with Cyclin B1-Cdk1, directs the accurate phosphorylation of multiple Cdk1 substrates such as Bub1, BubR1, Mps1, APC/C, and separase (Elowe *et al*, 2007; Morin *et al*, 2012b; Fujimitsu *et al*, 2016; Singh *et al*, 2021; Yu *et al*, 2021). With accumulating evidence to support the function of Cyclin B1 and B2 at kinetochores, it becomes clear that Cdk1 not only triggers mitotic signaling cascades, but also regulates multiple levels of cyto-architecture organization to facilitate mitotic progression, which includes

kinetochore assembly and reorganization, microtubule attachment, SAC, and separase activity.

In summary, our study uncovered a previously uncharacterized function of Cyclin B2 at the kinetochore. The Mad2-mediated kinetochore localization of Cyclin B2 safeguards faithful chromosome segregation. Currently, we are delineating how Cyclin B1-Cdk1 and Cyclin B2-Cdk1 signaling cascades cross-talk and synergize for accurate mitosis.

Materials and Methods

Cell culture, stable cell line screening, and drug treatments

HeLa, HCT116, and HEK293T cells (American Type Culture Collection) were cultured in DMEM (Gibco) with 10% (v/v) FBS (HyClone) and penicillin-streptomycin (100 units/ml and 100 µg/ml, respectively; Gibco) at 37°C in a humidified atmosphere with 8% CO₂. To generate lentivirus expressing GFP-Cyclin B1/B2, pLVX-EGFP-B1/B2 was co-transfected into 293T cells together with pMD2.G and psPAX2 plasmids. At 48 h after transfection, the supernatant was used to infect HeLa cells. GFP-Cyclin B1 and GFP-Cyclin B2-stable HeLa cell lines were selected and maintained in DMEM-containing puromycin (2.5 µg/ml). Nocodazole was used at 100 ng/ml, thymidine at 2.5 mM, the Eg5 inhibitor STLC at 10 µM, Taxol at 2 µM, the Cdk1 inhibitor RO-3306 at 10 µM, the Mps1 inhibitor reversine at 0.5 µM, and the Aurora B inhibitor hesperadin at 0.1 µM. For some experiments, 20-µM MG132 was added to synchronize cells at metaphase.

Plasmids, RNAi, and transfection

To generate GFP-tagged and GST-tagged full-length Cyclin B1, Cyclin B2, and their deletion mutants, PCR-amplified Cyclin B1, Cyclin B2 cDNA, or fragments were cloned into the pEGFP-C1 vector, the pLVX-EGFP-C1 vector, or the pGEX-6p-1 vector by ClonExpress Entry One Step Cloning Kit (Vazyme). To generate Flag-tagged and Trx-His-tagged Mad2 and its deletion mutants, PCR-amplified Mad2 cDNA or fragments were cloned into the 3×FLAG-Myc-CMV-24 vector and the pET.32 M.3C (gift by Prof. Chao Wang, USTC) vector by ClonExpress Entry One Step Cloning Kit (Vazyme). Site-specific mutants of Cyclin B2 and Mad2 were generated by Mut Express II Fast Mutagenesis Kits (Vazyme). All plasmids with the desired insertions and mutations were sequenced at General Biosystems.

Mad2 siRNA (GUCGGGACCACAGUUUAUU), Mad1 siRNA (CCAAAGUGCUGACAUGAG; CUCACCUUGUGAAUAAAA), Cyclin B1 siRNA (AAAUGUACCCUCCAGAAA), and Cyclin B2 siRNA (AGCAAACUCCUGAAGAUCA) were synthesized by GenePharma (Shanghai). All the expression plasmids were transfected using Lipofectamine3000 according to the manufacturer's protocol (Invitrogen). All siRNA duplexes were transfected using RNAiMAX (Invitrogen).

Antibodies

Rabbit anti-Cyclin B2 (Abcam, #ab185622, 1:1,000 for IF), mouse anti-Cyclin B2 (Santa Cruz, #sc-28303, 1:500 for WB), rabbit anti-Cyclin B2 (Proteintech, #21644-1-AP, 1:1,000), rabbit anti-Cyclin B1 (Cell Signaling Technology, CST, #12231, 1:1,000 for WB), mouse

anti- α -tubulin (Sigma, DM1A, 1:5,000 for WB), mouse anti- β -actin (Servicebio, #GB15001, 1:1,000 for WB), anti-centromere antibodies (ACA; Immuno-Vision, #HCT-0100, 1:5,000 for IF), mouse anti-Mad2 (Santa Cruz, #sc-65492, 1:200 for IF), mouse anti-Mad2 (Santa Cruz, #sc-47747, 1:100 for WB), mouse anti-Mad1 (Santa Cruz, #sc-65494, 1:200 for IF), rabbit anti-pericentrin (Abcam, #ab4448, 1:2,000 for IF), mouse anti-Nup107 (Abcam, mAb414, ab24609, 1:1,000 for IF), rabbit anti-Cdc20 (CST, #14866, 1:1,000 for WB/IF), mouse anti-BubR1 (BD, #612502, 1:1,000 for WB/IF), mouse anti-Bub1 antibody (Abcam, #ab54893, 1:500 for IF), mouse anti-Bub3 (Santa Cruz, #sc-376506, 1:1,000 for WB/IF), mouse anti-Flag (Sigma, #F1804, 1:2,000 for WB), mouse anti-His-tag (CST, #2366, 1:2,000 for WB), and rabbit anti-phospho-CDK substrate motif (CST, #9477, 1:1,000 for WB) were obtained commercially. For all Western blotting, signals were detected using HRP-conjugated anti-mouse or anti-rabbit antibodies (Jackson ImmunoResearch).

Immunofluorescence microscopy, image processing, and quantification

Unless indicated specifically, HeLa cells grown on coverslips were fixed and permeabilized simultaneously with PTEMF buffer [50 mM PIPES (pH 6.8), 0.2% Triton X-100, 10 mM EGTA, 1 mM MgCl₂, 4% formaldehyde] at room temperature and were processed for indirect immunofluorescence microscopy. Samples were examined with a DeltaVision microscope (Applied Precision) with a 60 \times objective lens, NA = 1.42, with optical sections acquired 0.2 μ m apart in the z axis. Deconvoluted images from each focal plane were projected into a single picture using softWoRx (Applied Precision). Images were taken at identical exposure times within each experiment and were acquired as 16-bit gray-scale images. After deconvolution, the images were exported as 24-bit RGB images and processed in Adobe Photoshop. Images shown in the same panel were identically scaled. Kinetochores intensities were measured in ImageJ (rsb.info.nih.gov/ij/) on non-deconvoluted images. The levels of kinetochores-associated proteins were quantified as described previously (Gui *et al*, 2020). In brief, the average pixel intensities from at least 20 kinetochores pairs from each cell were measured, and background pixel intensities were subtracted. The pixel intensities at each kinetochores pair were then normalized against ACA pixel values to account for any variations in staining or image acquisition. In all plots, each dot represents one cell. All *P*-values were calculated using the Student's *t*-test with Prism software (GraphPad).

To stain endogenous Cyclin B2, cells were rinsed for 1 min with PHEM buffer [100 mM PIPES, 20 mM HEPES (pH 6.9), 5 mM EGTA, 2 mM MgCl₂, and 4 M glycerol] and permeabilized for 1 min with PHEM plus 0.1% Triton X-100 as described (Yao *et al*, 1997). Extracted cells were then fixed in 4% formaldehyde in PHEM for 10 min and then rinsed three times in PBS.

Live-cell imaging

HeLa cells were cultured in glass-bottomed culture dishes (MatTek). During imaging, cells were cultured at 37°C in CO₂-independent medium (Invitrogen) containing 10% FBS and 2 mM glutamine and were observed with the DeltaVision RT system (Applied Precision).

Images were prepared for publication using Adobe Photoshop software.

Recombinant protein expression and GST pulldown assay

Glutathione S-transferase (GST) fusion proteins were expressed in bacteria BL21-Gold (DE3) strain and purified by using glutathione agarose as reported previously (Zhao *et al*, 2010). Briefly, the plasmids were transformed into an *E. coli* strain, and protein expression was induced with 0.2 mM IPTG at 16°C. Bacterially recombinant GST-tagged proteins were lysed by sonication in PBS-containing protease inhibitor cocktail (Sigma, #P8849), followed by incubation with Glutathione Sepharose 4B (GE Healthcare Life Science) for 1 h at 4°C. Different 6 \times His-Mad2 fusion proteins were purified using Ni-NTA beads (Qiagen) according to the manufacturer's protocol. GST-tagged Cyclin B1 (165–433) and Cyclin B2 (135–398) fusion protein-bound glutathione beads were incubated with purified 6 \times His-Mad2 fusion proteins in PBS buffer containing 0.1% Triton X-100 plus 1 mM PMSF and 1 mM DTT for 2.5 h at 4°C. After the incubation, the beads were washed three times with PBS containing 0.1% Triton X-100 and once with PBS and boiled in SDS-PAGE sample buffer. The bound proteins were then separated on 10% SDS-PAGE. In parallel, the samples were analyzed by an anti-His tag antibody using Western blots.

Immunoprecipitation and Western Blots

HEK293T cells or HeLa cells were collected and lysed in IP buffer (50 mM HEPES, pH 7.4; 150 mM NaCl; 2 mM MgCl₂; 1 mM EGTA; 0.2% Triton X-100; 1 mM DTT) supplemented with protease inhibitor cocktail (Sigma, #P8340). Cell lysates were clarified by centrifugation at 12,000 rpm for 20 min at 4°C. For different purposes, clarified cell lysates were incubated with FLAG-M2 resin (Sigma) for 2 h before washing. The binding fraction was washed with IP buffer three times before being resolved by SDS-PAGE and immunoblotted with indicated antibodies.

Samples were separated by standard SDS-PAGE electrophoresis, then transferred to nitrocellulose membranes. Western blotting was performed using standard protocols. For all Western blotting, signals were detected using HRP-conjugated anti-mouse or anti-rabbit antibodies (Pierce) through use of a Fuji ImageQuant LAS 400 machine.

MS sample preparation and analysis

The Flag immunoprecipitation and wash conditions were described in "Immunoprecipitation and pulldown assay". After washing, the samples were reduced with 10 mM DTT in 50 mM ammonium bicarbonate at 56°C for 30 min and then alkylated with 30 mM iodoacetamide for 30 min. Afterwards, 2 μ g of trypsin (Promega, V511A) was added to samples for overnight digestion at 37°C. After trypsin digestion, the peptide samples were desalted and analyzed with a Thermo Fisher Q Exactive mass spectrometer equipped with Easy-nanoLC, followed by a scan range of *m/z* 350–1550. The raw files were analyzed with Thermo Proteome Discoverer (1.4.1.14). The human database was from Uniprot (Proteome ID: UP000005640). Phosphorylation (S/T, +79.9663 Da) and oxidation (M, +15.9949 Da) modifications were included as variable modifications. Carbamidomethyl (C, +57.0215 Da) was set as a fix modification.

Online supplemental materials

Figure EV1 provides data on subcellular localization of Cyclin B2 in cell cycle. Figure EV2 provides data on localization of endogenous Cyclin B2 in cells treated with different mitotic kinase inhibitors and physical interaction between Cyclin B2 and Mad2. Figure EV3 provides data on Cyclin B1 and Cyclin B2 localization in cells depleted of Mad1. Figure EV4 provides chromosome segregation phenotype of HCT116 cells with knocked-down Cyclin B2. Figure EV5 provides data on localization of Mad1, Bub1, and BubR1 in cells treated with control siRNA or Cyclin B2 siRNA. Datasets EV1–EV4 provide the mass spectrometry results of Flag-Cyclin B1 and B2 immunoprecipitation.

Data availability

No data were deposited in a public database.

Expanded View for this article is available online.

Acknowledgements

We thank C. Wang for reagents and all members in our laboratories for helpful discussions. This work was supported by the National Key Research and Development Program of China (2017YFA0503600, 2017YFA0102900, and 2016YFA0100500), the National Natural Science Foundation of China (31621002, 32090040, 91854203, 32170733, 31671407, 31871359, 21922706, 91853115, 92153302, 92053104, and 22177106); the Ministry of Education (IRT_17R102); Anhui province Natural Sciences Foundation grant (2108085J15); the Strategic Priority Research Program of the Chinese Academy of Sciences (XDB19040000); and the Fundamental Research Funds for the Central Universities (WK2070000066 and WK2070000194).

Author contributions

Sikai Liu: Data curation; Formal analysis; Investigation; Writing—review & editing. **Xiao Yuan:** Data curation; Formal analysis. **Ping Gui:** Formal analysis; Investigation. **Ran Liu:** Formal analysis; Investigation. **Olanrewaju Ayodeji Durojaye:** Formal analysis. **Donald L Hill:** Writing—review & editing. **Chuanhai Fu:** Data curation; Writing—review & editing. **Xuebiao Yao:** Conceptualization; Supervision; Funding acquisition; Writing—original draft; Project administration; Writing—review & editing. **Zhen Dou:** Conceptualization; Data curation; Supervision; Funding acquisition; Investigation; Writing—original draft; Project administration; Writing—review & editing. **Xing Liu:** Supervision; Funding acquisition; Writing—original draft; Writing—review & editing.

In addition to the CRediT author contributions listed above, the contributions in detail are:

XYa and ZD involved in conceptualization. SL, XYu, PG, RL, and ZD involved in investigation. SL, XYu, OD, ZD, and XYa involved in investigation. XL, ZD, CF, DLH, and XYa involved in manuscript writing. XL, ZD, and XYa involved in funding acquisition. ZD, XYa, and XL involved in supervision.

Disclosure and competing interests statement

The authors declare that they have no conflict of interest.

References

Alfonso-Perez T, Hayward D, Holder J, Gruneberg U, Barr FA (2019) MAD1-dependent recruitment of CDK1-CCNB1 to kinetochores promotes spindle checkpoint signaling. *J Cell Biol* 218: 1108–1117

Allan LA, Camacho Reis M, Ciossani G, Huis In't Veld PJ, Wohlgemuth S, Kops GJ, Musacchio A, Saurin AT (2020) Cyclin B1 scaffolds MAD1 at the kinetochore corona to activate the mitotic checkpoint. *EMBO J* 39: e103180

Bentley AM, Normand G, Hoyt J, King RW (2007) Distinct sequence elements of cyclin B1 promote localization to chromatin, centrosomes, and kinetochores during mitosis. *Mol Biol Cell* 18: 4847–4858

Brandeis M, Rosewell I, Carrington M, Crompton T, Jacobs MA, Kirk J, Gannon J, Hunt T (1998) Cyclin B2-null mice develop normally and are fertile whereas cyclin B1-null mice die in utero. *Proc Natl Acad Sci USA* 95: 4344–4349

Chen Q, Zhang X, Jiang Q, Clarke PR, Zhang C (2008) Cyclin B1 is localized to unattached kinetochores and contributes to efficient microtubule attachment and proper chromosome alignment during mitosis. *Cell Res* 18: 268–280

Choi E, Zhang X, Xing C, Yu H (2016) Mitotic checkpoint regulators control insulin signaling and metabolic homeostasis. *Cell* 166: 567–581

Clijsters L, van Zon W, Riet BT, Voets E, Boekhout M, Ogink J, Rumpf-Kienzl C, Wolthuis RM (2014) Inefficient degradation of cyclin B1 re-activates the spindle checkpoint right after sister chromatid disjunction. *Cell Cycle* 13: 2370–2378

Cohen-Sharir Y, McFarland JM, Abdusamad M, Marquis C, Bernhard SV, Kazachkova M, Tang H, Ippolito MR, Laue K, Zerbib J et al (2021) Aneuploidy renders cancer cells vulnerable to mitotic checkpoint inhibition. *Nature* 590: 486–491

Crnec A, Hochegger H (2019) Triggering mitosis. *FEBS Lett* 593: 2868–2888

Daldello EM, Luong XG, Yang CR, Kuhn J, Conti M (2019) Cyclin B2 is required for progression through meiosis in mouse oocytes. *Development* 146: dev172734

D'Angiolella V, Mari C, Nocera D, Rametti L, Grieco D (2003) The spindle checkpoint requires cyclin-dependent kinase activity. *Genes Dev* 17: 2520–2525

Dou Z, Prifti DK, Gui P, Liu X, Elowe S, Yao X (2019) Recent progress on the localization of the spindle assembly checkpoint machinery to kinetochores. *Cells* 8: 278

Draviam VM, Orrechia S, Lowe M, Pardi R, Pines J (2001) The localization of human cyclins B1 and B2 determines CDK1 substrate specificity and neither enzyme requires MEK to disassemble the Golgi apparatus. *J Cell Biol* 152: 945–958

Elowe S, Hummer S, Uldschmid A, Li X, Nigg EA (2007) Tension-sensitive Plk1 phosphorylation on BubR1 regulates the stability of kinetochore microtubule interactions. *Genes Dev* 21: 2205–2219

Fujimitsu K, Grimaldi M, Yamano H (2016) Cyclin-dependent kinase 1-dependent activation of APC/C ubiquitin ligase. *Science* 352: 1121–1124

Gallant P, Nigg EA (1992) Cyclin B2 undergoes cell cycle-dependent nuclear translocation and when expressed as a non-destructible mutant, causes mitotic arrest in HeLa cells. *J Cell Biol* 117: 213–224

Gascoigne KE, Cheeseman IM (2013) CDK-dependent phosphorylation and nuclear exclusion coordinately control kinetochore assembly state. *J Cell Biol* 201: 23–32

Gong D, Ferrell Jr JE (2010) The roles of cyclin A2, B1, and B2 in early and late mitotic events. *Mol Biol Cell* 21: 3149–3161

Gong D, Pomerening JR, Myers JW, Gustavsson C, Jones JT, Hahn AT, Meyer T, Ferrell Jr JE (2007) Cyclin A2 regulates nuclear-envelope breakdown and the nuclear accumulation of cyclin B1. *Curr Biol* 17: 85–91

Gui L, Homer H (2013) Hec1-dependent cyclin B2 stabilization regulates the G2-M transition and early prometaphase in mouse oocytes. *Dev Cell* 25: 43–54

Gui P, Sedzro DM, Yuan X, Liu S, Hei M, Tian W, Zohbi N, Wang F, Yao Y, Aikhionbare FO et al (2020) Mps1 dimerization and multisite interactions

- with Ndc80 complex enable responsive spindle assembly checkpoint signaling. *J Mol Cell Biol* 12: 486–498
- Hara M, Fukagawa T (2018) Kinetochore assembly and disassembly during mitotic entry and exit. *Curr Opin Cell Biol* 52: 73–81
- Hauf S, Cole RW, LaTerra S, Zimmer C, Schnapp G, Walter R, Heckel A, van Meel J, Rieder CL, Peters JM (2003) The small molecule Hesperadin reveals a role for Aurora B in correcting kinetochore-microtubule attachment and in maintaining the spindle assembly checkpoint. *J Cell Biol* 161: 281–294
- Hayward D, Alfonso-Perez T, Cundell MJ, Hopkins M, Holder J, Bancroft J, Hutter LH, Novak B, Barr FA, Gruneberg U (2019a) CDK1-CCNB1 creates a spindle checkpoint-permissive state by enabling MPS1 kinetochore localization. *J Cell Biol* 218: 1182–1199
- Hayward D, Alfonso-Perez T, Gruneberg U (2019b) Orchestration of the spindle assembly checkpoint by CDK1-cyclin B1. *FEBS Lett* 593: 2889–2907
- Hégarat N, Crncec A, Suarez Peredo Rodriguez MF, Echegaray Iturra F, Gu Y, Busby O, Lang PF, Barr AR, Bakal C, Kanemaki MT et al (2020) Cyclin A triggers Mitosis either via the Greatwall kinase pathway or Cyclin B. *EMBO J* 39: e104419
- Hochegger H, Takeda S, Hunt T (2008) Cyclin-dependent kinases and cell-cycle transitions: does one fit all? *Nat Rev Mol Cell Biol* 9: 910–916
- Houston J, Lara-Gonzalez P, Desai A (2020) Rashomon at the kinetochore: function(s) of the Mad1-cyclin B1 complex. *J Cell Biol* 219: e202006006
- Jackman M, Firth M, Pines J (1995) Human cyclins B1 and B2 are localized to strikingly different structures: B1 to microtubules, B2 primarily to the Golgi apparatus. *EMBO J* 14: 1646–1654
- Jackman M, Lindon C, Nigg EA, Pines J (2003) Active cyclin B1-Cdk1 first appears on centrosomes in prophase. *Nat Cell Biol* 5: 143–148
- Jackman M, Marozzi C, Barbiero M, Pardo M, Yu L, Tyson AL, Choudhary JS, Pines J (2020) Cyclin B1-Cdk1 facilitates MAD1 release from the nuclear pore to ensure a robust spindle checkpoint. *J Cell Biol* 219
- Karasu ME, Bouftas N, Keeney S, Wassmann K (2019) Cyclin B3 promotes anaphase I onset in oocyte meiosis. *J Cell Biol* 218: 1265–1281
- Lara-Gonzalez P, Pines J, Desai A (2021) Spindle assembly checkpoint activation and silencing at kinetochores. *Semin Cell Dev Biol* 117: 86–98
- Li J, Ouyang YC, Zhang CH, Qian WP, Sun QY (2019) The cyclin B2/CDK1 complex inhibits separase activity in mouse oocyte meiosis I. *Development* 146: dev182519
- Li J, Tang J-X, Cheng J-M, Hu B, Wang Y-Q, Aalia B, Li X-Y, Jin C, Wang X-X, Deng S-L et al (2018) Cyclin B2 can compensate for Cyclin B1 in oocyte meiosis I. *J Cell Biol* 217: 3901–3911
- Li J, Zhang HY, Wang F, Sun QY, Qian WP (2021) The cyclin B2/CDK1 complex conservatively inhibits separase activity in oocyte meiosis II. *Front Cell Dev Biol* 9: 648053
- Li Y, Benzra R (1996) Identification of a human mitotic checkpoint gene: hsMAD2. *Science* 274: 246–248
- Luo X, Tang Z, Rizo J, Yu H (2002) The Mad2 spindle checkpoint protein undergoes similar major conformational changes upon binding to either Mad1 or Cdc20. *Mol Cell* 9: 59–71
- Luo X, Yu H (2008) Protein metamorphosis: the two-state behavior of Mad2. *Structure* 16: 1616–1625
- Malumbres M, Barbacid M (2005) Mammalian cyclin-dependent kinases. *Trends Biochem Sci* 30: 630–641
- Mapelli M, Massimiliano L, Santaguida S, Musacchio A (2007) The Mad2 conformational dimer: structure and implications for the spindle assembly checkpoint. *Cell* 131: 730–743
- Mo F, Zhuang X, Liu X, Yao PY, Qin BO, Su Z, Zang J, Wang Z, Zhang J, Dou Z et al (2016) Acetylation of Aurora B by TIP60 ensures accurate chromosomal segregation. *Nat Chem Biol* 12: 226–232
- Morin V, Prieto S, Melines S, Hem S, Rossignol M, Lorca T, Espeut J, Morin N, Abrieu A (2012a) CDK-dependent potentiation of MPS1 kinase activity is essential to the mitotic checkpoint. *Curr Biol* 22: 289–295
- Morin V, Prieto S, Melines S, Hem S, Rossignol M, Lorca T, Espeut J, Morin N, Abrieu A (2012b) CDK-dependent potentiation of MPS1 kinase activity is essential to the mitotic checkpoint. *Curr Biol* 22: 289–295
- Musacchio A (2015) The molecular biology of spindle assembly checkpoint signaling dynamics. *Curr Biol* 25: R1002–1018
- Nam HJ, van Deursen JM (2014) Cyclin B2 and p53 control proper timing of centrosome separation. *Nat Cell Biol* 16: 538–549
- Nigg EA (2001) Mitotic kinases as regulators of cell division and its checkpoints. *Nat Rev Mol Cell Biol* 2: 21–32
- Orth M, Mayer B, Rehm K, Rothweiler U, Heidmann D, Holak TA, Stemmann O (2011) Shugoshin is a Mad1/Cdc20-like interactor of Mad2. *EMBO J* 30: 2868–2880
- Pachis ST, Kops G (2018) Leader of the SAC: molecular mechanisms of Mps1/TTK regulation in mitosis. *Open Biol* 8: 180109
- Rattani A, Vinod PK, Godwin J, Tachibana-Konwalski K, Wolna M, Malumbres M, Novak B, Nasmyth K (2014) Dependency of the spindle assembly checkpoint on Cdk1 renders the anaphase transition irreversible. *Curr Biol* 24: 630–637
- Santaguida S, Tighe A, D'Alise AM, Taylor SS, Musacchio A (2010) Dissecting the role of MPS1 in chromosome biorientation and the spindle checkpoint through the small molecule inhibitor reversine. *J Cell Biol* 190: 73–87
- Santaguida S, Vernieri C, Villa F, Ciliberto A, Musacchio A (2011) Evidence that Aurora B is implicated in spindle checkpoint signalling independently of error correction. *EMBO J* 30: 1508–1519
- Satyanarayana A, Kaldis P (2009) Mammalian cell-cycle regulation: several Cdks, numerous cyclins and diverse compensatory mechanisms. *Oncogene* 28: 2925–2939
- Saurin AT, van der Waal MS, Medema RH, Lens SM, Kops GJ (2011) Aurora B potentiates Mps1 activation to ensure rapid checkpoint establishment at the onset of mitosis. *Nat Commun* 2: 316
- Singh P, Pesenti ME, Maffini S, Carmignani S, Hedtfeld M, Petrovic A, Srinivasamani A, Bange T, Musacchio A (2021) BUB1 and CENP-U, primed by CDK1, are the main PLK1 Kinetochore Receptors in mitosis. *Mol Cell* 81: 67–87.e9
- Soni DV, Sramkoski RM, Lam M, Stefan T, Jacobberger JW (2008) Cyclin B1 is rate limiting but not essential for mitotic entry and progression in mammalian somatic cells. *Cell Cycle* 7: 1285–1300
- Ubersax JA, Ferrell JE (2007) Mechanisms of specificity in protein phosphorylation. *Nat Rev Mol Cell Biol* 8: 530–541
- Vassilev LT, Tovar C, Chen S, Knezevic D, Zhao X, Sun H, Heimbrook DC, Chen L (2006) Selective small-molecule inhibitor reveals critical mitotic functions of human CDK1. *Proc Natl Acad Sci USA* 103: 10660–10665
- Vazquez-Novelle MD, Sansregret L, Dick AE, Smith CA, McAinsh AD, Gerlich DW, Petronczki M (2014) Cdk1 inactivation terminates mitotic checkpoint surveillance and stabilizes kinetochore attachments in anaphase. *Curr Biol* 24: 638–645
- Xu L, Ali M, Duan W, Yuan X, Garba F, Mullen McKay, Sun B, Poser I, Duan H, Lu J et al (2021) Feedback control of PLK1 by Apol1 ensures accurate chromosome segregation. *Cell Rep* 36: 109343

- Yao X, Anderson KL, Cleveland DW (1997) The microtubule-dependent motor centromere-associated protein E (CENP-E) is an integral component of kinetochore corona fibers that link centromeres to spindle microtubules. *J Cell Biol* 139: 435–447
- Yu H, Yao X (2008) Cyclin B1: conductor of mitotic symphony orchestra. *Cell Res* 18: 218–220
- Yu J, Raia P, Ghent CM, Raisch T, Sadian Y, Cavadini S, Sabale PM, Barford D, Raunser S, Morgan DO et al (2021) Structural basis of human separase regulation by securin and CDK1-cyclin B1. *Nature* 596: 138–142
- Zhao L, Jin C, Chu Y, Varghese C, Hua S, Yan F, Miao Y, Liu J, Mann D, Ding X et al (2010) Dimerization of CPAP orchestrates centrosome cohesion plasticity. *J Biol Chem* 285: 2488–2497